International Journal of Pharmaceutics 577 (2020) 119033

Contents lists available at ScienceDirect

International Journal of Pharmaceutics

journal homepage: www.elsevier.com/locate/ijpharm

Nanostructured lipid carriers-mediated brain delivery of carbamazepine for improved *in vivo* anticonvulsant and anxiolytic activity

Namrah Khan[a], Fawad Ali Shah[a], Isra Rana[a], Muhammad Mohsin Ansari[a], Fakhar ud Din[b], Syed Zaki Husain Rizvi[a], Waqar Aman[c], Gwan-Yeong Lee[d], Eun-Sun Lee[d], Jin-Ki Kim[d,*], Alam Zeb[a,*]

[a] Riphah Institute of Pharmaceutical Sciences, Riphah International University, Islamabad, Pakistan
[b] Department of Pharmacy, Quaid-i-Azam University, Islamabad, Pakistan
[c] Faculty of Pharmacy, University of Central Punjab, Lahore, Pakistan
[d] College of Pharmacy, Institute of Pharmaceutical Science and Technology, Hanyang University, Ansan, Gyeonggi, Republic of Korea

ARTICLE INFO

Keywords:
Carbamazepine
Nanostructured lipid carriers
Brain delivery
Anticonvulsant activity
Anxiolytic activity

ABSTRACT

The limited brain delivery of carbamezapine (CBZ) presents a major hurdle in the successful epilepsy treatment. The potential of carbamezapine-loaded nanostructured lipid carriers (CBZ-NLCs) for improved brain delivery is investigated in the current study. CBZ-NLCs were prepared by using binary mixture of trilaurin and oleic acid as a lipid core stabilized with Poloxamer 188, Tween 80 and Span 80. CBZ-NLCs were evaluated for physicochemical properties, *in vitro* release, *in vivo* brain kinetics, anticonvulsant and anxiolytic activities. The optimized CBZ-NLCs demonstrated nanometric particle size (97.7 nm), surface charge of −22 mV and high drug incorporation (85%). CBZ-NLCs displayed biphasic release pattern with initial fast followed by sustained drug release. CBZ-NLCs significantly enhanced the AUC of CBZ (520.4 μg·h/mL) in brain compared with CBZ dispersion (244.9 μg·h/mL). *In vivo* anticonvulsant activity of CBZ-NLCs in PTZ-induced seizure model showed a significant increase in the onset time (143.0 sec) and reduction in duration (17.2 sec) of tonic-clonic seizures compared with CBZ dispersion (75.4 and 37.2 sec). The anxiolytic activity in light-dark box and elevated-plus maze models also demonstrated superiority of CBZ-NLCs to CBZ dispersion. From the results, CBZ-NLCs presents a promising strategy to improve brain delivery and therapeutic outcomes of CBZ in epilepsy.

1. Introduction

Epilepsy is one of the frequently occurring brain disease described by spontaneous recurrent seizures, affecting approximately 50 million people globally with ~5 million new diagnosis each year (WHO, 2019). The clinical applications of antiepileptic drugs are hampered because of drug resistance and treatment discontinuation, thereby making it difficult to manage seizures (Wiebe and Jette, 2012). It was reported that around 20–25% of the patients do not respond to antiepileptic therapy due to drug resistance, which results in about 7-folds higher mortality rate in resistant patients (Sperling, 2004). Carbamazepine (CBZ) is an antiepileptic and anxiolytic drug widely used to treat seizures, trigeminal neuralgia and bipolar disorders (Elmowafy et al., 2018). The anticonvulsant activity of CBZ results from blockage of sodium channel activity thereby modulating release of excitatory neurotransmitters (Ambrosio et al., 2002). CBZ shows its anxiolytic activity by modulating adenosine mediated neurotransmitters to alter postsynaptic ionic current (Van Calker et al., 1991). On the basis of Biopharmaceutics Classification System, CBZ is categorized as class II drug with high permeability (log P = 2.45) and poor aqueous solubility of 113 μg/mL at room temperature (Kumar and Siril, 2014; Sethia and Squillante, 2002). The poor aqueous solubility and extensive hepatic metabolism is manifested as slow, variable and dissolution rate-dependent absorption of CBZ after oral administration (Landmark et al., 2012; Sethia and Squillante, 2002). Formulating injectable dosage form of CBZ is also a challenging task owing to poor aqueous solubility. In addition to solubility-related problems, one of the major obstacle in effective brain delivery is the presence of blood-brain barrier (BBB) which restricts majority of large molecules (100%) and small (98%) to access the brain (Gabathuler, 2010; Zeb et al., 2019b). The BBB comprises of vascular

* Corresponding authors at: College of Pharmacy, Institute of Pharmaceutical Sciences and Technology, Hanyang University, 55 Hanyangdaehak-ro, Sangnok-gu, Ansan, Gyeonggi 15588, Republic of Korea (J.-K. Kim). Riphah Institute of Pharmaceutical Science, Riphah International University, Sector G-7/4, 7th Avenue, Islamabad 44000, Pakistan (A. Zeb).

E-mail addresses: jinkikim@hanyang.ac.kr (J.-K. Kim), alam.zeb@riphah.edu.pk (A. Zeb).

https://doi.org/10.1016/j.ijpharm.2020.119033
Received 3 October 2019; Received in revised form 20 December 2019; Accepted 11 January 2020
Available online 16 January 2020
0378-5173/

Table 1
Optimization parameters, composition and physicochemical properties of CBZ-NLCs.

Composition (mg)								Physicochemical properties				
Code	TL	OA	P 188	Tw 80	Sp 80	CBZ	HLB	PS (nm)	PDI	ZP (mV)	IE (%)	LC (%)
F1	6.65	0.35	14	70	9.24	5.25	16.03	149.1 ± 4.1	0.31 ± 0.87	−24.5 ± 3.2	73.6 ± 1.2	3.70 ± 0.06
F2	5.95	1.05	14	70	9.24	5.25	16.03	108.9 ± 2.3	0.44 ± 0.98	−20.0 ± 2.1	77.2 ± 1.5	3.88 ± 0.08
F3	4.9	2.1	14	70	9.24	5.25	16.03	97.7 ± 1.2	0.27 ± 0.04	−22.0 ± 1.5	85.0 ± 2.6	4.26 ± 0.13
F4	3.5	3.5	14	70	9.24	5.25	16.03	89.8 ± 2.4	0.42 ± 0.10	−12.6 ± 1.6	65.1 ± 0.6	3.29 ± 0.03
Blank	4.9	2.1	14	70	9.24	–	16.03	95.2 ± 1.0	0.19 ± 0.01	−21.8 ± 1.3	–	–

TL; trilaurin, OA; oleic acid, P 188; Poloxamer 188, Tw 80; Tween 80, Sp 80, Span 80, CBZ; carbamazepine, HLB; hydrophilic-lipophilic balance, PS; particle size, PDI; polydispersity index, ZP; zeta potential, IE; incorporation efficiency, LC; loading content.
Data are expressed as mean ± S.D. (n = 3).

endothelial cells firmly connected by tight junctions, adherens, a scanty layer of pericytes and perivascular astrocytes (Saraiva et al., 2016). The permeability of drugs into the brain via paracellular and transcellular pathways is limited by the protective functions of tight junctions and efflux transporters (prominently Pgps and MRPs), respectively (Baratchi et al., 2009; Kwan and Brodie, 2005). The limited permeability of CBZ across the BBB and overexpression of efflux pumps hamper the optimal therapeutic response for the effective management of epilepsy (Zybina et al., 2018).

In the recent past, nanotechnology has produced a number of nanoparticulate platforms that are capable of tuning the basic features and bioactivity of drugs. These nanoplatforms have improved the drug transport to brain apart from the advantages of improved biological and chemical stability, modulation of drug release profile, reduced toxicity, feasibility of incorporating hydrophilic and lipophilic drugs and administration through various routes (Din et al., 2017; Goldsmith et al., 2014; Sim et al., 2016). Nanostructured lipid carriers (NLCs) are the second generation of lipid nanoparticles consisting of binary mixture of solid and liquid lipids. NLCs offer higher payload and reduced drug expulsion compared to their first generation counterparts composed of solid lipid alone. The imperfections created by liquid lipids help to accommodate high payload and reduce drug expulsion by preventing polymorphic transitions of solid lipid from less ordered to highly ordered crystal structure (Müller et al., 2002). Most prominently, NLCs have the inherent capability, because of their lipid nature and small size, to penetrate the BBB even without any surface functionalization (Tapeinos et al., 2017). Few studies have been reported for the application of lipid-based nanoparticles in the brain delivery of CBZ. However, main foci of the earlier studies were either to improve the oral bioavailability and thereby pharmacodynamics compared with conventional CBZ suspension and marketed product (Elmowafy et al., 2018), or to investigate the *in vitro* cell permeability and *in vivo* anticonvulsant activity compared with CBZ solution in animal models (Scioli Montoto et al., 2018). These reports lack sufficient evidence to indicate the improved brain delivery of CBZ across BBB. The direct measurement of CBZ in brain tissues (brain kinetics) along with *in vivo* anticonvulsant and anxiolytic activities would truly reflect the therapeutic potential of CBZ-loaded nanostructured lipid carriers (CBZ-NLCs) in brain delivery.

The present study aims to explore the potential of CBZ-NLCs for improved brain delivery for the management of epilepsy and anxiety in experimental animals. CBZ-NLCs were optimized by varying the amount of solid lipid, lipid lipids and surfactants, followed by characterization for physicochemical properties and *in vitro* release. *In vivo* brain kinetic study was performed in rats to determine the concentration of CBZ reaching brain at various intervals. In addition, anticonvulsant and anxiolytic activities of CBZ-NLCs were determined in appropriate pharmacodynamic animal models.

2. Materials and methods

2.1. Materials

Carbamazepine (CBZ) was kindly gifted by Valor Pharma. Co., Ltd. (Islamabad, Pakistan). Pentylenetetrazol (PTZ), trilaurin, oleic acid, Tween 80, Span 80 and Poloxamer 188 were obtained from Sigma Aldrich (St. Louis, MO, USA). All other chemicals used in the current study were of analytical grade and were used without further purification.

2.2. Preparation of CBZ-NLCs

CBZ-NLCs were prepared by utilizing nano-emulsion template technique with slight modification (Rizvi et al., 2019; Scioli Montoto et al., 2018). Briefly, mixture of lipids (trilaurin and oleic acid) and surfactants (Tween 80, Span 80 and Poloxamer 188) was melted in a water bath at 70 °C. CBZ dissolved in DMSO was added to molten mixture of lipids and surfactants followed by heating at 70 °C with continuous stirring to evaporate DMSO. A clear nano-emulsion was obtained when the preheated deionized water was added to the above mixture with continuous stirring at 800 rpm for 30 min. To obtain CBZ-NLCs, the lipid core was solidified by rapid cooling-down process in ice bath. The large aggregates and unloaded drug were removed from CBZ-NLCs by passing the formulation through a 0.45 µm PVDF syringe filter. The formulations were stored at 4 °C until further analysis. The composition of CBZ-NLCs with various lipids and surfactants is presented in Table 1.

2.3. Physicochemical characterization of CBZ-NLCs

2.3.1. Particle size, polydispersity index, zeta potential and incorporation efficiency

The average particle size, polydispersity index (PDI) and zeta potential of prepared CBZ-NLCs were determined with a Zetasizer ZS 90 (Malvern Instruments, Malvern, Worcestershire, UK). The formulations were suitably diluted with filtered deionized water before the analysis. The analysis was performed at room temperature and a scattering angle of 90° using Zetasizer software version 6.34 (Din et al., 2019). The incorporation efficiency of CBZ-NLCs was determined by spectrophotometric analysis (Elmowafy et al., 2018). CBZ-NLCs devoid of the large aggregates and unloaded CBZ were dissolved in methanol and analyzed for drug contents by using UV–visible spectrophotometer at 287 nm (V-530; JASCO Corporation, Tokyo, Japan). The incorporation efficiency and loading content of CBZ-NLCs was calculated as follow;

$$\text{Incorporation efficiency (\%)} = \frac{\text{weight of CBZ in CBZ} - \text{NLCs}}{\text{total weight of CBZ added}} \times 100$$

$$\text{Loading content } (\%) = \frac{\text{weight of CBZ in CBZ} - \text{NLCs}}{\text{total weight of CBZ} - \text{NLCs}} \times 100$$

2.3.2. Transmission electron microscopy (TEM)

The surface morphology of optimized CBZ-NLCs was evaluated using field-emission transmission electron microscopy (JEM-2100F; JEOL, Tokyo, Japan). The formulation was suitably diluted and allowed to adsorb on the surface of 400-mesh carbon-coated copper grid. The surface adsorbed CBZ-NLCs were negatively stained with 1% phosphotungstic acid solution followed by drying at room temperature. The dried grid was imaged using TEM operated at an accelerating voltage of 200 kV (Zeb et al., 2016).

2.3.3. Differential scanning calorimetry (DSC)

DSC was carried out to investigate the thermal behavior of lyophilized CBZ-NLCs and their individual solid components using differential scanning calorimeter (DSC Q20; TA Instrument, New Castle, DE, USA). CBZ-NLCs were lyophilized without cryoprotectant using a freeze-dryer (TFD5503, IlShin BioBase Co., Ltd. Gyeonggido, Republic of Korea). Samples were heated in sealed aluminum pans over a range of 0–250 °C at the rate of 10 °C/min.

2.3.4. Powder X-ray diffractometry (PXRD)

The lyophilized CBZ-NLCs and their solid components were assessed for X-ray diffraction patterns using a powder X-ray diffractometer (D8 Advance-Bruker, Billerica, MA, USA). Samples were scanned in the 2θ range from 3° to 70° at 0.02°/s of scanning rate. The operating current and voltage were maintained at 40 mA and 40 kV, respectively (Qureshi et al., 2017).

2.3.5. Fourier transform infrared spectroscopy (FTIR)

FTIR spectroscopy of CBZ-NLCs was carried to characterize the molecular dynamics of formulation and its individual solid components. The infrared spectra were obtained in the range of 4000–400 cm^{-1} at a resolution of 4 cm^{-1} using attenuated total reflectance Fourier transform infrared spectrophotometer (Eco Alpha II- Bruker, Billerica, MA, USA).

2.4. In vitro release studies

In vitro release of CBZ from CBZ-NLCs was evaluated by using dialysis membrane diffusion technique. Dialysis membrane was soaked in the release medium for 15 min before the experiment. CBZ-NLCs formulation equivalent to 5 mg of CBZ was placed in dialysis membrane having molecular cut-off weight of 3500 Da (Spectrum Laboratories, Inc., Rancho Dominguez, CA, USA). The dialysis membrane was immersed in 500 mL phosphate buffer saline (pH 7.4) containing 0.1% (w/v) Tween 80 to maintain sink condition (Liu et al., 2018). The release media was maintained at 37 ± 0.5 °C and continuously stirred at 100 rpm. Aliquots of 2 mL were withdrawn from the release medium at predetermined intervals for 24 h. An equal volume of fresh buffer was immediately added to maintain constant volume of release medium. The acquired samples were then analyzed spectrophotometrically at 287 nm for the determination of CBZ contents.

2.5. Experimental animals

The *in vivo* plasma and brain kinetics were conducted in male Sprague Dawley rats (200 ± 20 g), while anticonvulsant and anxiolytic activities were conducted in male mice (20 ± 5 g). The animals were obtained from the National Institute of Health (Islamabad, Pakistan) and retained in standard conditions to acclimatize them with the laboratory environment. Experimental studies on animals were approved by Research and Ethics Committee of Riphah Institute of Pharmaceutical Sciences and were in line with NIH policy and animal welfare act.

2.6. In vivo plasma and brain kinetics of CBZ-NLCs

2.6.1. Administration of CBZ-NLCs to rats

The rats were randomly assigned to CBZ-NLCs and CBZ dispersion groups (30 rats each) and kept on fasting for 12 h before the administration of each formulation. Each group of rats was either administered CBZ-NLCs or CBZ dispersion at a dose equivalent to 10 mg/kg of CBZ via intraperitoneal injection (Barakat et al., 2006). Blood samples (0.6 mL) were collected via cardiac puncture at time intervals of 0.5, 1, 1.5, 2, 4, 6, 8, 12, 18 and 24 h, respectively. The collected blood samples were centrifuged at 3000 g for 15 min to separate plasma and stored at −20 °C for further analysis. Rats were sacrificed after blood collection and brain of each rat was removed, rinsed with normal saline and stored at −80 °C for further analysis.

2.6.2. Analysis of CBZ in plasma and brain samples

The isolated plasma or homogenized brain samples were analyzed for the determination of CBZ concentration by HPLC. The plasma or brain homogenate (0.3 mL) was mixed with ethyl acetate (6 mL) followed by the addition of 50 µL of diclofenac sodium solution (10 µg/mL) as an internal standard. The mixture was vortexed for 2 min and subsequently centrifuged at 3000 g for 15 min (Barakat et al., 2006). The supernatant was separated and the organic layer was allowed to evaporate in a rotary evaporator at 45 °C (N-1200BS Series, Rikakikai Co., Ltd. Tokyo, Japan). The obtained residue was reconstituted with 100 µL of the mobile phase, filtered through 0.45 µm syringe filter and analyzed with HPLC system (Agilent 1260 Infinity, Agilent Technologies; Santa Clara, CA, USA) equipped with an auto-sampler and Hypersil Gold C_{18} analytical column (150 × 4.6 mm dimensions with 5 µm particle size, Thermo Scientific, Waltham, MA, USA). The HPLC conditions for CBZ measurement comprised of methanol and water (50:50, v/v) as the mobile phase, flow rate of 1 mL/min, injection volume of 20 µL, column temperature of 25 °C and UV detector wavelength of 287 nm.

2.6.3. Determination of pharmacokinetic parameters

Non-compartmental analysis was performed with WinNonlin™ software (Version 5.2, Scientific Consulting Inc., Apex, NC, USA) to determine various plasma and brain kinetic parameters including maximum concentration (C_{max}), area under the concentration-time curve ($AUC_{0\rightarrow\infty}$), area under first moment curve ($AUMC_{0\rightarrow\infty}$) and mean residence time (MRT).

2.6.4. Calculation of brain distribution parameters

The effectiveness of both formulations for brain delivery was evaluated by calculating various brain distribution parameters including brain targeting index and brain enhancement factor (Wen et al., 2011). Brain targeting index describes brain to plasma CBZ concentration ratio for CBZ-NLCs or CBZ dispersion at specific time interval. Brain enhancement factor is the ratio of CBZ concentration in brain achieved by CBZ-NLCs to that of CBZ dispersion.

2.7. In vivo anticonvulsant activity of CBZ-NLCs

The anticonvulsant activity of CBZ-NLCs was evaluated in PTZ-induced seizures mice model (Khan et al., 2016). Mice were randomly divided into four groups (n = 5), receiving an intraperitoneal injection of normal saline (10 mL/kg), diazepam (2 mg/kg), CBZ dispersion (10 mg/kg) and CBZ-NLCs (10 mg/kg). After 30 min, each mouse was injected with PTZ solution at a dose of 90 mg/kg via intraperitoneal route. The mice were subsequently observed for onset time of myoclonic jerks, onset time and duration of tonic-clonic seizures (Mesdaghinia et al., 2019). Mortality rate (%) in mice was also calculated for each group.

2.8. In vivo anxiolytic activity of CBZ-NLCs

The anxiolytic activity of CBZ-NLCs was evaluated in light-dark box and elevated-plus maze models in mice (Khan et al., 2016). Light-dark apparatus comprises of a rectangular wooden box (44 × 21 × 21 cm) divide into two compartments covered with wooden lids. A smaller dark compartment (1/3) is painted in black and a bigger light compartment (2/3) is painted in white and illuminated with a 60 Watt bulb. The light and dark compartments are separated by a wooden board having an opening of 7 × 7 cm at its base to allow the movement of mice from one compartment to another (Bourin and Hascoët, 2003). Mice were randomly divided to four groups (n = 5) and were given a daily dose of normal saline (10 mL/kg), diazepam (2 mg/kg), CBZ dispersion (10 mg/kg) and CBZ-NLCs (10 mg/kg) via intraperitoneal route for 7 days. Following 30 min of daily injection, mice were placed in the light-dark box and the time spent in each compartment was recorded for 5 min.

Elevated-plus maze model is based on a wooden apparatus having two open arms (30 × 5 cm) with slightly raised edges (3 mm high and 1 mm thick) and two closed arms (30 × 5 × 15 cm). The apparatus is mounted 40 cm above the ground with open and closed arms of apparatus joined together by a central compartment (5 × 5 cm) (Karim et al., 2012). For elevated-plus maze, mice were randomly divided to four groups (n = 5) and were given a daily dose of normal saline (10 mL/kg), diazepam (2 mg/kg), CBZ dispersion (10 mg/kg) and CBZ-NLCs (10 mg/kg) via intraperitoneal route for 7 days. Following 30 min of daily injection, mice were placed in the central compartment of elevated-plus maze apparatus and entry as well as residence time of mice in open and closed arms were recorded for 5 min.

2.9. Statistical analysis

The experiments were conducted with a minimum of three independent replicates and results are expressed as the mean ± standard deviation (S.D.) or standard error of mean (S.E.M). The statistical significance among the groups were calculated by comparing their means through student's *t*-test, or one-way ANOVA with post hoc Tukey test using SPSS software (SPSS Inc., Chicago, IL, USA) at a p value < 0.05.

3. Results and discussion

3.1. Preparation and optimization of CBZ-NLCs

NLCs represents a versatile class of lipid nanoparticles comprised of solid and liquid lipids combination, sterically stabilized by surfactant shell (Müller et al., 2002; Zeb et al., 2019a). As drug delivery carriers, NLCs offer a number of advantages over polymeric or inorganic nanoparticles such as better tolerability, improved drug stability and efficacy, and high drug encapsulation (Din et al., 2017). The excellent tolerability of NLCs results from the use of biocompatible, biodegradable and non-toxic lipids, and pharmaceutically acceptable surfactants of GRAS (generally regarded as safe) category as Poloxamer 188, Tween 80 and Span 80 (Ana et al., 2019). In the context of brain delivery, lipid nature and small size of NLCs make them superior for penetrating the BBB even without any surface functionalization (Tapeinos et al., 2017).

CBZ-NLCs were effectively and reproducibly prepared by nano-template method, which involves development of nanoemulsion to be used as a template for nanoparticles formation. The method is advantageous as it avoids the use of extensive mechanical mixing and excessive organic solvents (Anton et al., 2008). Trilaurin and oleic acid were respectively utilized as solid and liquid lipids for the preparation of CBZ-NLCs. Trilaurin is a medium chain triglyceride having three 12-C lauric acid units with a melting point of 46.5 °C. Trilaurin possesses lower melting point and aqueous viscosity than its higher C-chains counterparts such as tripalmitin and tristearin resulting in a smaller particle size (Qureshi et al., 2016). The addition of oleic acid as a liquid lipid creates imperfections in the lipid core, thereby accommodates more drug in lattice (Müller et al., 2002). A mixture of nonionic and biocompatible surfactants consisting of Poloxamer 188, Tween 80 and Span 80 was used to stabilize CBZ-NLCs. It has been reported that a blend of surfactants with different HLB values tend to provide better stability to nano-emulsions than that provided by a single surfactant (Qureshi et al., 2017)

In the preliminary experiments, cumulative hydrophilic-lipophilic balance (HLB) values of surfactant mixture was varied between 15 and 18 (Supplementary material). Optimal particle size, PDI, zeta potential and incorporation efficiency of CBZ-NLCs was achieved at the HLB value of 16.03. The cumulative HLB value of surfactants play a vital role to ensure optimum stability and properties of nanoparticulate systems. The O/W emulsions are usually stabilized efficiently with the emulsifier system having HLB values in the range of 8–18 (Zheng et al., 2015). After fixing HLB of surfactants mixture at 16.03, the amounts of solid and liquid lipids were varied between 95/5, 85/15, 70/30 and 50/50 (%) of the total lipid core. The incorporation efficiency was significantly increased (72.8% to 85.2%) when the amount of oleic acid was increased from 5% to 30% (F1 vs. F3) of the total lipid core (Table 1). The addition of oleic acid as a liquid lipid increased the incorporation of CBZ in the lipid core due to the formation of highly disordered crystal lattice (Hu et al., 2005). Further increase in the amount of oleic acid to 50% (F4) of the lipid core resulted in a substantial decrease in the incorporation efficiency (65.1%) of CBZ-NLCs. This could be ascribed to reduced immobilization of lipid core and subsequently decreased drug-retaining capacity at higher liquid lipid proportions (Zeb et al., 2017). Taken together, CBZ-NLCs with trilaurin/oleic acid at 70/30 (w/w) ratio (F3) showed optimum particle size, PDI and zeta potential with the highest incorporation efficiency and loading content. The formulation, F3, was therefore selected for further characterization, *in vitro* release study and *in vivo* evaluation.

3.2. Physicochemical properties and morphology of CBZ-NLCs

The physicochemical properties of nanoparticles affect their ability of penetrating BBB in brain delivery. The optimized formulation of CBZ-NLCs displayed an average particle size of 97.7 ± 1.2 nm and PDI value of 0.27 ± 0.04 (Table 1). Nanoparticles have shown size-dependent permeation across BBB with the smallest particles being the most effective (Etame et al., 2011). The particles between 50 and 100 nm are the most frequently investigated and desirable nanoparticles for brain delivery in animal models (Saraiva et al., 2016). Low PDI value (0.27) and unimodal distribution curve (Fig. 1A) demonstrate the homogeneity of CBZ-NLCs since PDI < 0.3 generally indicates homogeneous distribution of particles (Zhang et al., 2009). The optimized CBZ-NLCs showed negatively charged surface with zeta potential of −22 ± 1.5 mV. Zeta potential values of around −30 mV create an electrorepulsion and ensure the physical stability of nanoparticles by preventing their aggregation (Estella-Hermoso de Mendoza et al., 2009). In addition, highly negatively charged particles (−15 to −45 mV) are superior to their positively charged counterparts in brain drug delivery as they might compromise the integrity of BBB (Lockman et al., 2004). The optimized CBZ-NLCs showed high incorporation efficiency (85%) and loading content (4.26%) which is significant for minimizing the administration volume of injectable formulation and preventing the toxicity arising from the use of excessive excipients. Consequently, the aqueous solubility of CBZ increased 7.89 folds in CBZ-NLCs (from 113 μg/mL to 892 μg/mL). TEM image described smooth and spherical morphology with uniform distribution of CBZ-NLCs (Fig. 1B). The particle size of around 100 nm revealed by TEM analysis corresponds well to that measured by dynamic light scattering.

3.3. Solid state characterization of CBZ-NLCs

Thermal attributes of lyophilized CBZ-NLCs and their solid

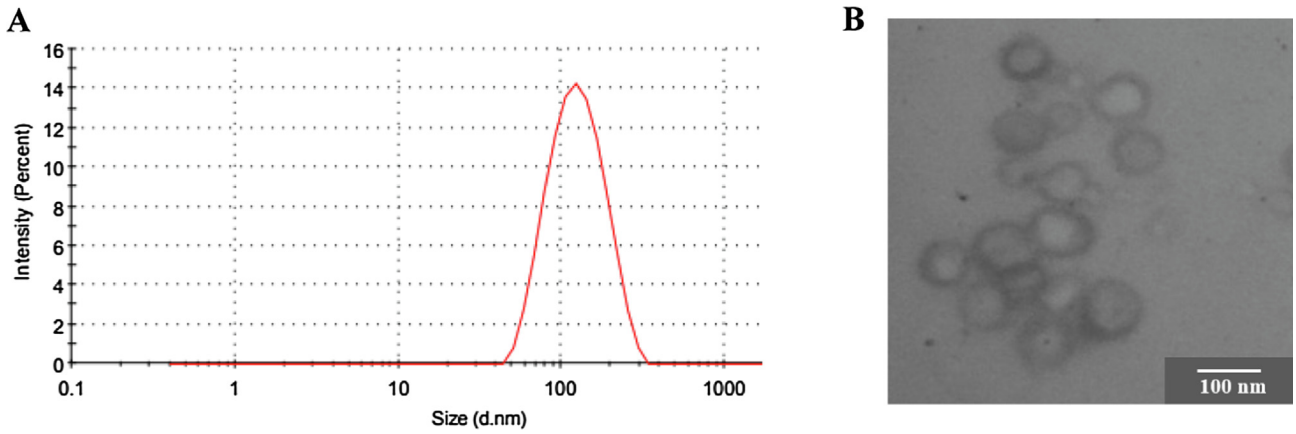

Fig. 1. Particle size distribution curve (A) and TEM image (B) of CBZ-NLCs.

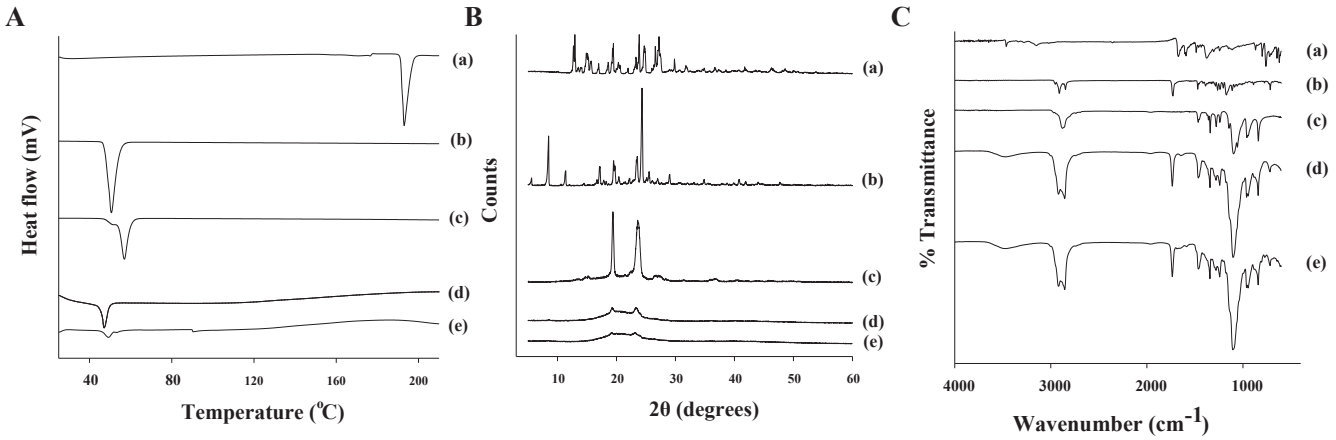

Fig. 2. DSC thermograms (A), PXRD diffractograms (B) and FTIR spectra (C) of CBZ (a), trilaurin (b), Poloxamer 188 (c), blank NLCs (d) and CBZ-NLCs (e).

components were evaluated by DSC to observe changes in crystallinity and drug-lipid interactions. DSC thermograms are presented in Fig. 2A, indicating sharp endothermic peaks at ~93 °C, 49.8 °C and 56 °C for CBZ (a), trilaurin (b) and Poloxamer 188 (c) corresponding to their respective melting points. In contrary, blank NLCs (d) and CBZ-NLCs (e) displayed slightly suppressed and broadened endothermic peaks between 47 and 49 °C which could be ascribed to the melting of lipid matrix. The disappearance of sharp melting peak at ~193 °C in DSC curve of CBZ-NLCs is attributed to molecular dispersion of amorphous CBZ in the lipid core (Islan et al., 2016). The shifting of trilaurin melting peak to a slightly lower temperature in blank NLCs and CBZ-NLCs might be due to the incorporation of oleic acid into lipid matrix, the interaction of lipid phase with surfactant mixture and Kelvin effect produced from small particle size (Lv et al., 2009; Rizvi et al., 2019). In addition, the interaction between solid and liquid lipids results in the formation of amorphous regions in the lipid matrix, thereby facilitating molecular dispersion of incorporated drug (Islan et al., 2016). From DSC results, the absence of sharp melting peak of CBZ in the thermogram of CBZ-NLCs confirmed its conversion from native crystalline state into amorphous state.

The crystalline attributes of lyophilized CBZ-NLCs and their components were further ascertained by PXRD (Fig. 2B). The PXRD pattern of CBZ (a) demonstrated characteristics crystalline peaks at 2θ equals to 13.08°, 19.62°, 23.84° and 27.19°. The crystalline nature of trilaurin was confirmed by observing peaks at 8.46°, 19.62°, 23.65° and 24.37° (b). Similarly, Poloxamer 188 showed crystalline peaks at 19.5° and 23.54° (c). However, sharp peaks of CBZ were missing in the PXRD patterns of CBZ-NLCs proposing the loss of crystallinity of CBZ in the lipid matrix of CBZ-NLCs. The crystalline nature of trilaurin is also diminished as shown by reduction in the intensity and position of its peaks in blank NLCs and CBZ-NLCs. Overall, good correlation was found between PXRD and DSC in the lost and reduced crystallinity for CBZ and trilaruin, respectively.

The molecular interactions of CBZ with lipid matrix were further investigated by FTIR analysis and the spectra obtained in the range of 4000–400 cm^{-1} is presented in Fig. 2C. The fundamental peaks of CBZ were observed at 3496 cm^{-1} for NH_2 group and C=O amide stretch at 1680 cm^{-1} with multiple peaks at 1607, 1491 and 1391 cm^{-1} (a) for aromatic rings. Spectrum of trilaurin (b) showed characteristic C=O ester peak at 1735 cm^{-1} and long alkyl chain (1472–1120 cm^{-1}), while Poloxamer 188 (c) displayed characteristic −OH stretch at 2889 cm^{-1}. The characteristics peaks of CBZ were disappeared in the spectrum for CBZ-NLCs indicating the successful incorporation of CBZ in the lipid core. The incorporation of CBZ into lipid matrix of CBZ-NLCs resulted in the loss of its crystallinity as evidenced by missing sharp peaks in DSC thermograms, PXRD diffractograms and FTIR spectra (Chen et al., 2008; Qureshi et al., 2017).

3.4. *In vitro* release profile of CBZ-NLCs

The *in vitro* release of CBZ from CBZ-NLCs was evaluated in phosphate buffer saline as a release medium (pH 7.4) maintained at the body temperature (37 °C), and was compared with that of CBZ dispersion. Since CBZ possess poor aqueous solubility, the release medium was therefore added with 0.1% Tween 80 to maintain sink conditions by dissolving the released amount of drug (Rizvi et al., 2019). CBZ-NLCs displayed a biphasic drug release profile with a slightly faster CBZ release (~28%) in the initial 4 h, followed by comparatively slower and

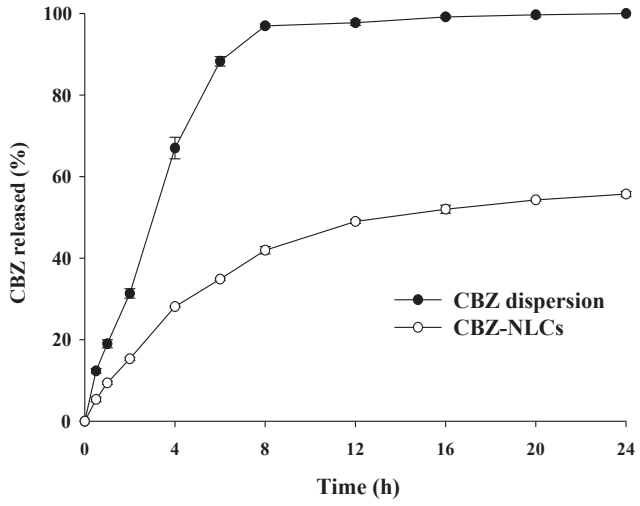

Fig. 3. *In vitro* release profile of CBZ-NLCs and CBZ dispersion in phosphate buffer saline (pH 7.4) for 24 h at 37 °C. Data are expressed as mean ± S.D. (n = 3).

sustained release of CBZ (~57%) for 24 h (Fig. 3). The initial faster release could be explained on the basis of accumulation of CBZ in liquid lipid-enriched outer shell of CBZ-NLCs. The liquid lipid-enriched shell is formed when the molten lipid mixture is rapidly cooled down to prepare NLCs (Hu et al., 2005). During cooling process, trilaurin is solidified first owning to its higher melting point thereby forming solid lipid-enriched layer followed by the formation of oleic acid-enriched outer layer. CBZ in the softer oleic acid-enriched layer is easily and quickly released by diffusion and surface erosion resulting in the initial higher release rate from CBZ-NLCs (Zeb et al., 2017). Compared with CBZ-NLCs, *in vitro* drug release rate from CBZ dispersion was substantially faster as 67% and 99% of CBZ released after 4 h and 24 h, respectively. The delayed CBZ release from CBZ-NLCs could be ascribed to the retention of incorporated drug in lipid matrix and the barrier effect of surfactant mixture layer (Qureshi et al., 2016; Üner and Yener, 2007).

3.5. Chromatographic analysis of CBZ in plasma and brain

The concentration of CBZ in plasma and brain samples was measured by HPLC analysis. The chromatographic separation of CBZ and diclofenac sodium (internal standard) was effectively achieved on Hypersil Gold C_{18} analytical column (150 mm length, 4.6 mm inner diameter, Thermo Scientific, Waltham, MA, USA) at room temperature. The internal standard and CBZ peaks appeared at the retentions times of 4.471 and 6.812 min, respectively (Fig. 4A). The calibration curves of CBZ were constructed with plasma and brain samples, supplemented with known amounts of diclofenac sodium as an internal standard, by plotting CBZ concentrations against the respective peak area ratios of CBZ to the internal standard. The obtained calibration curves of CBZ were linear over the concentration range of 1.25–40 μg/mL with correlation coefficient (R^2) values of 0.9997 and 0.9998 for plasma and brain, respectively (Fig. 4B and C). The concentrations of CBZ in plasma and brain samples at different time intervals were determined by using with the respective linear regression equations. The results indicated that the developed method was effective to separate and detect CBZ without having any interfering peak near its retention time.

3.6. Pharmacokinetic and brain distribution profiles of CBZ-NLCs

The plasma and brain kinetic behaviours of CBZ-NLCs was evaluated and compared with those of CBZ dispersion following single intraperitoneal injection to rats. The plasma and brain concentration *versus* time curves of CBZ-NLCs and CBZ dispersion are presented in Fig. 5A and B, respectively. CBZ-NLCs resulted in a higher concentration of CBZ in plasma and brain at each time point than CBZ dispersion. As shown in Table 2, $AUC_{0\rightarrow\infty}$, $AUMC_{0\rightarrow\infty}$ and C_{max} of CBZ-NLCs is plasma were 1.36, 1.45 and 1.43-folds than those of CBZ dispersion, respectively. On the other hand, AUC0→∞ in brain significantly increased when CBZ-NLCs were administered instead of CBZ dispersion (520.4 vs 244.9 μg·h/mL). Moreover, the brain concentrations of CBZ-NLCs at same time points were much higher than its plasma concentrations. To evaluate brain targeting potential of CBZ-NLCs, various brain distribution parameters were calculated including brain targeting index and brain enhancement factor (Table 3). The higher brain distribution of CBZ for CBZ-NLCs was substantially demonstrated by its brain targeting index. Similarly, CBZ-NLCs increased the brain enhancement factor of CBZ by 1.35–5 folds compared with dispersion. Overall, these results suggest the enhanced brain accumulation of CBZ via CBZ-NLCs-mediated delivery through BBB.

Several mechanisms could be suggested for the enhanced permeation of CBZ across BBB when CBZ-NLCs were administered. Small particle size (< 100 nm), large surface area and lipophilic nature of CBZ-NLCs increase contact time with BBB and facilitate their transport into the brain accompanied by generating drug concentration gradient (He et al., 2016; Kaur et al., 2008; Wong et al., 2010). It has also been reported that endocytosis, transcytosis and opening of tight junctions between the endothelial cells contribute to nanoparticles-mediated transport of drugs across BBB (Saraiva et al., 2016; Zeb et al., 2019b). Surfactants in CBZ-NLCs could cause membrane fluidization, improved interaction with BBB and inhibition of efflux pumps located on the brain endothelial cells, thereby enhancing brain delivery by nanoparticles (Blasi et al., 2007; Kaur et al., 2008). In addition, the presence of surfactants such as Tween 80 and Poloxamer 188 not only increase the permeability of BBB but also facilitate the binding to lipoprotein receptors via adsorption to plasma proteins and transporting into the brain (Lim et al., 2014). The combined effects of these mechanisms might be attributed to improved brain delivery of CBZ-NLCs.

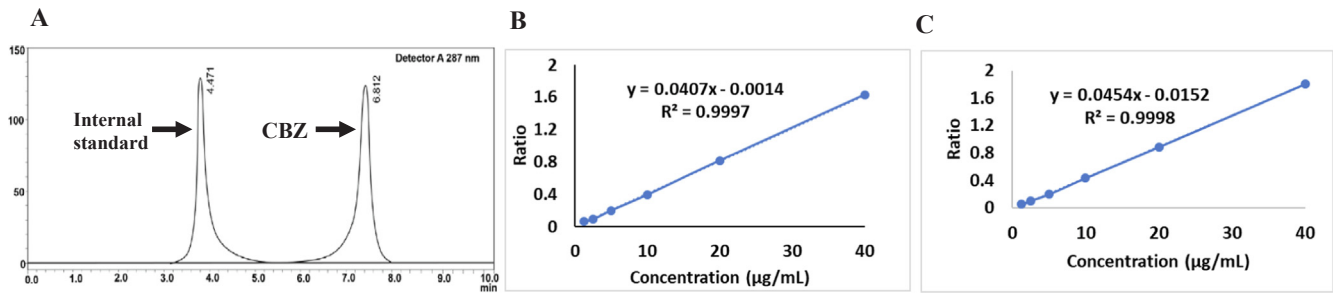

Fig. 4. HPLC analysis of CBZ in plasma and brain samples. Chromatogram of CBZ at the optimal HPLC conditions (A), and calibration curves of CBZ with plasma (B) and brain (C).

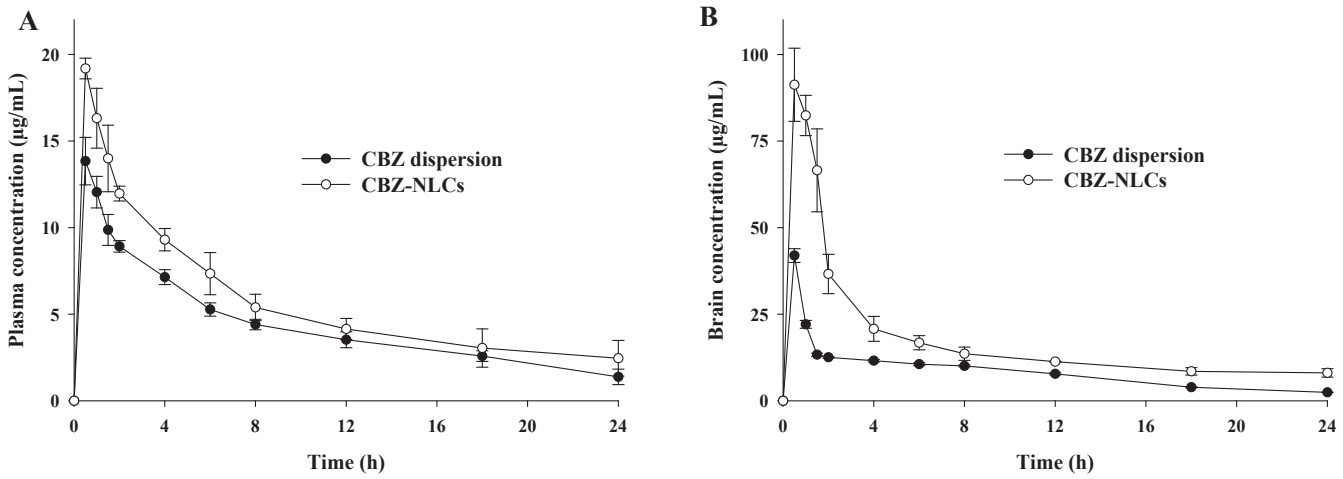

Fig. 5. Average plasma concentration *versus* time curve (A) and average brain concentration *versus* time curve (B) of CBZ after intraperitoneal administration of CBZ-NLCs and CBZ dispersion (equivalent to 10 mg/kg of CBZ) to rats. Data are expressed as mean ± S.D. (n = 3).

Table 2
Pharmacokinetic parameters in plasma and brain after i.p administration of CBZ-NLCs and CBZ dispersion (equivalent to 10 mg/kg of CBZ).

Parameters	Plasma		Brain	
	CBZ dispersion	CBZ-NLCs	CBZ dispersion	CBZ-NLCs
$AUC_{0\rightarrow\infty}$ (μg·h/mL)	126.5 ± 14.9	171.8 ± 34.7	244.9 ± 0.8	520.4 ± 36.4**
$AUMC_{0\rightarrow\infty}$ (μg·h^2/mL)	1540.0 ± 478.1	2230.7 ± 102.4	2509.0 ± 69.4	5869.5 ± 955.9**
MRT (h)	12.0 ± 2.3	12.5 ± 3.5	10.2 ± 0.3	11.2 ± 1.1
C_{max} (μg/mL)	15.9 ± 2.2	22.7 ± 1.5*	80.0 ± 6.8	101.4 ± 17.5

$AUC_{0\rightarrow\infty}$; area under the plasma and brain concentration-time curve up to time infinity, AUMC; area under first moment curve, MRT; mean residence time, C_{max}; peak plasma and brain concentrations.
Data are expressed as mean ± S.D. (n = 3). *$p < 0.05$ *versus* CBZ dispersion in plasma and **$p < 0.01$ *versus* CBZ dispersion in brain. The statistical significance was calculated by student's *t*-test.

Table 3
Brain distribution parameters after i.p administration of CBZ-NLCs and CBZ dispersion.

Time (h)	Brain targeting index		Brain enhancement factor
	CBZ dispersion	CBZ-NLCs	
0.5	3.06 ± 0.42	4.77 ± 0.70*	2.18 ± 0.23
1	1.84 ± 0.22	5.09 ± 0.68*	3.73 ± 0.13
1.5	1.36 ± 0.16	4.76 ± 0.69*	5.01 ± 0.90
2	1.41 ± 0.08	3.07 ± 0.57*	2.92 ± 0.47
4	1.62 ± 0.07	2.22 ± 0.23*	1.79 ± 0.27
6	2.01 ± 0.16	2.30 ± 0.21	1.59 ± 0.25
8	2.30 ± 0.21	2.52 ± 0.14	1.35 ± 0.19
12	2.24 ± 0.36	2.76 ± 0.41	1.45 ± 0.06
18	1.53 ± 0.21	3.01 ± 0.91*	2.18 ± 0.35
24	1.89 ± 0.57	3.60 ± 0.20*	3.32 ± 0.60

$\text{Brain targeting index} = \frac{\text{CBZ concentration in brain}}{\text{CBZ concentration in plasma}}$.

$\text{Brain enhancement factor} = \frac{\text{Brain concentration for CBZ – NLCs}}{\text{Brain concentration for CBZ dispersion}}$.

Data are expressed as mean ± S.D. (n = 3). *p value < 0.05 *versus* CBZ dispersion at corresponding time interval. The statistical significance was calculated by student's *t*-test.

3.7. Anticonvulsant activity of CBZ-NLCs

The anticonvulsant activity of CBZ-NLCs was assessed in PTZ-induced seizure mice model. PTZ inhibits γ-aminobutyric acid to induce seizures and it is a widely accepted and utilized as experimental animal model to evaluate effectiveness of anticonvulsant drugs (Li et al., 2014). The effects of CBZ-NLCs treatment on the onset time and duration of myoclonic jerks and tonic-clonic seizures are presented in Fig. 6. The results showed that CBZ-NLCs significantly delayed the onset time of myoclonic jerks (97.20 ± 4.66 sec) compared with mice treated with saline (39.2 ± 3.19 sec) and CBZ dispersion (62.20 ± 3.11 sec). Similarly, delayed onset time and reduced duration of tonic-clonic seizures were observed in CBZ-NLCs-treated group (143.0 ± 5.14 and 17.20 ± 4.76 sec) compared to saline- (56.80 ± 3.27 and

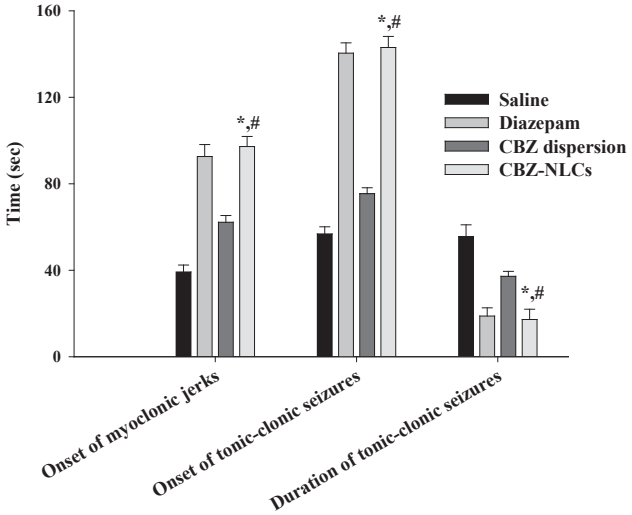

Fig. 6. Effects of CBZ-NLCs on the onset time of myoclonic jerks, tonic-clonic seizures and duration for tonic-clonic seizures in PTZ-induced seizure mice model. Data are expressed as mean ± S.D. (n = 5). *$p < 0.01$ *versus* saline and #$p < 0.01$ *versus* CBZ dispersion. The statistical significance was calculated by one-way ANOVA with post hoc Tukey test.

Table 4
Mortality rate in mice after CBZ-NLCs administration in PTZ-induced anticonvulsant activity.

Groups	Mortality rate (%)
Saline (10 mL/kg) + PTZ (90 mg/kg)	100.0
Diazepam (2 mg/kg) + PTZ (90 mg/kg)	0.0*
CBZ dispersion (10 mg/kg) + PTZ (90 mg/kg)	40.0*
CBZ-NLCs (10 mg/kg) + PTZ (90 mg/kg)	0.0*#

Data expressed as mean ± S.D. (n = 5). *$p < 0.01$ *versus* saline and #$p < 0.01$ *versus* CBZ dispersion. The statistical significance was calculated by student's *t*-test.

55.60 ± 5.41 sec) and CBZ dispersion- (75.40 ± 2.72 and 37.20 ± 2.28 sec) treated groups, respectively. It is noteworthy to mention that the anticonvulsant activity of CBZ-NLCs was comparable to diazepam control in terms of onset time of myoclonic jerks (92.60 ± 5.50 sec), onset of tonic-clonic seizures (140.4 ± 4.77 sec) and duration of tonic-clonic seizures (18.80 ± 3.81 sec). Diazepam is a member of benzodiazepines family and widely used as positive control in PTZ-induced seizure model due to its effectiveness in epilepsy (Chen et al., 2011). Mortality rate (%) of mice in PTZ-induced seizures was also monitored in all treatment groups and the results are summarized in Table 4. The survival rate of CBZ-NLCs- and diazepam-treated groups was 100% whereas saline- and CBZ dispersion-treated groups showed 100% and 40% mortality rate, respectively. These results demonstrate effective management of seizures in CBZ-NLCs- and diazepam-treated groups. The improved anticonvulsant activity of CBZ-NLCs could be attributed to their efficient brain delivery and in agreement to the brain kinetic results.

3.8. Anxiolytic activity of CBZ-NLCs

The anxiolytic activity of CBZ-NLCs was investigated in light-dark box mice model. The light-dark box is a widely used model based on inborn tendency of mice to avoid illuminated areas and exhibit spontaneous locomotor behaviours when exposed to stressful condition of novel environment and light (Bourin and Hascoët, 2003). The specially constructed box allowed mice to explore two interlinked compartments with different sizes (2 and 1), colors (white and black) and illumination (bright and dim). The time spent by mice in light and dark compartments using light-dark box model are presented in Fig. 7A. Saline-treated mice spent less time in light compartment (92.62 ± 1.72 sec) than in dark compartment (210.57 ± 8.05 sec) owing to their natural tendency to avoid bright areas in anxious conditions. In contrary, CBZ-NLCs treatment significantly increased the residence time of mice in light compartment to 135.66 ± 4.04 sec and decreased the time spent in dark compartment to 139.66 ± 8.08 sec. The anxiolytic effects of CBZ-NLCs were comparable with diazepam-treated mice having mean residence time of 138.63 ± 5.69 and 135.06 ± 3.05 sec in light and dark compartments, respectively. On the other hand, CBZ dispersion-treated group only showed a slight change in residence time of mice in light compartment (114.0 ± 4.04 sec) and in dark compartment (173.0 ± 6.24 sec) in comparison to saline-treated group. These results indicate the anxiolytic effects were improved by CBZ-NLCs presumably having efficient delivery of CBZ into brain.

The anxiolytic activity of CBZ-NLCs was further assessed by using elevated-plus maze model. The elevated-plus maze model is one of the most popular behavioural anxiety model and used to investigate the potential of anxiolytic drugs in mice (Bourin, 2015). It is based on natural propensity of mice towards enclosed dark spaces (secure) and fear for open and elevated spaces (unsecure), thereby producing unconditional anxiety responses. The anxiolytic behaviour is characterized by increased entries and duration in open arm. Unlike elevated-plus maze model, light-dark box model measures conditional behavioural responses upon the presentation of anxious stimulus (Walf and Frye, 2007). The behavioural responses of mice were quantified in terms of time spent and number of entries to closed and open arms of elevated-plus maze apparatus as presented in Fig. 7B and C, respectively. Saline-treated mice showed more time spent (235.58 ± 7.56 sec) and number of entries (18.0 ± 1.0) to closed arms than those to open arms (25.70 ± 0.74 sec and 6.33 ± 0.57), respectively. Treatment with CBZ-NLCs significantly increased the open arm activities (89.33 ± 4.90 sec and 12.88 ± 0.50) and reduced the time spent (134.66 ± 5.50 sec) and number of entries (7.33 ± 0.57) to closed arms compared with saline-treated group. Diazepam-treated mice spent 95.80 ± 1.87 and 124.52 ± 1.48 sec in open and closed arms with 13.66 ± 1.52 and 6.66 ± 0.57 entries to open and closed arms, respectively. CBZ-NLCs displayed comparable anxiolytic effects with that of diazepam used as a control in this study. Although CBZ dispersion treatment increased time spent (68.35 ± 1.09 sec) and number of entries (9.66 ± 0.57) to open arms and reduced these parameters in closed arms (172.95 ± 3.53 sec and 10.0 ± 1.0, respectively), the anxiolytic effects of CBZ-NLCs and diazepam were higher than those of CBZ dispersion. Taken together, the improved anxiolytic activity in light-dark box and elevated-plus maze models could be ascribed to effective modulation of excitatory neurotransmitters owing to efficient brain delivery mediated by CBZ-NLCs.

4. Conclusion

The efficient and specific brain delivery of CBZ is required to achieve optimal therapeutic outcomes in epilepsy. In this study, the potential of nanostructured lipid carriers prepared with biocompatible and biodegradable ingredients was investigated to overcome the limited CBZ delivery to the brain. The optimized CBZ-NLCs enabled high drug incorporation (85%) with 7.9-folds increase in CBZ aqueous

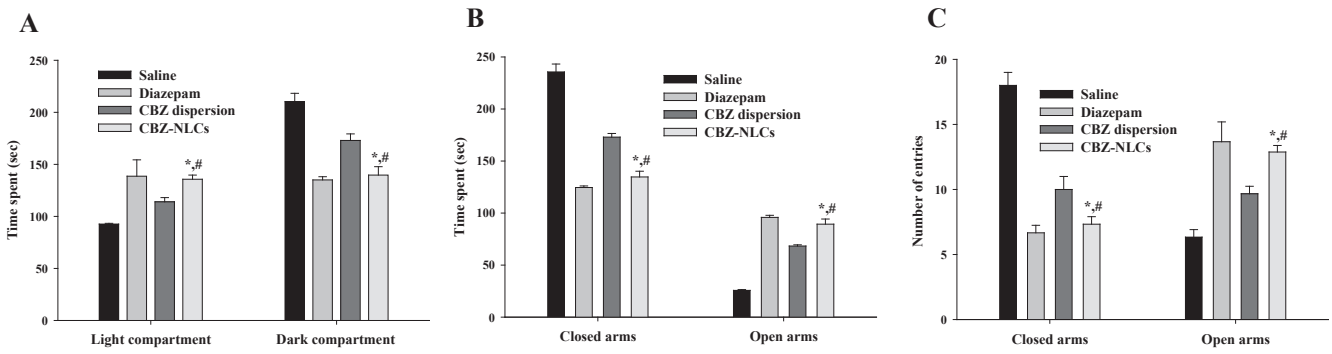

Fig. 7. Effects of CBZ-NLCs on the time spent in light and dark compartments in light-dark box mice model (A), the time spent (B) and number of entries (C) in open and closed arms in elevated plus maze mice model. Data are expressed as mean ± S.D. (n = 5). *$p < 0.01$ *versus* saline and #$p < 0.01$ *versus* CBZ dispersion. The statistical significance was calculated by one-way ANOVA with post hoc Tukey test.

solubility. CBZ-NLCs significantly improved brain deposition of CBZ coupled with enhanced *in vivo* anticonvulsant and anxiolytic activities compared with CBZ dispersion. Consequently, NLCs-mediated brain drug delivery suggests a promising strategy that will open up new perspective for the treatment of neurological diseases.

Disclosure

The authors report no conflict of interest in this work.

CRediT authorship contribution statement

Namrah Khan: Conceptualization, Data curation, Formal analysis, Investigation, Methodology, Writing - original draft, Writing - review & editing. **Fawad Ali Shah:** Conceptualization, Data curation, Writing - review & editing. **Isra Rana:** Conceptualization, Formal analysis, Writing - review & editing. **Muhammad Mohsin Ansari:** Data curation, Supervision, Resources, Software, Writing - review & editing. **Fakhar ud Din:** Data curation, Writing - review & editing. **Syed Zaki Husain Rizvi:** Formal analysis, Writing - review & editing. **Waqar Aman:** Investigation, Methodology, Writing - review & editing. **Gwan-Yeong Lee:** Investigation, Methodology, Writing - review & editing. **Eun-Sun Lee:** Investigation, Methodology, Writing - review & editing. **Jin-Ki Kim:** Funding, Project administration, Supervision, Resources, Software, Writing - original draft, Writing - review & editing. **Alam Zeb:** Funding, Project administration, Supervision, Resources, Software, Writing - original draft, Writing - review & editing.

Declaration of Competing Interest

The authors declare that they have no known competing financial interests or personal relationships that could have appeared to influence the work reported in this paper.

Acknowledgements

The authors are grateful to the Higher Education Commission of Pakistan for their financial support (grant No: 21-1590/SRGP/R&D/HEC/2017) and the Basic Science Research Program of National Research Foundation of Korea (NRF) funded by the Ministry of Science and ICT (NRF-2017R1A2B4006458). Riphah Academy of Research and Education is also acknowledged for partial support through seed money grant program of Riphah International University.

Appendix A. Supplementary material

Supplementary data to this article can be found online at https://doi.org/10.1016/j.ijpharm.2020.119033.

References

Ambrosio, A.F., Soares-Da-Silva, P., Carvalho, C.M., Carvalho, A.P., 2002. Mechanisms of action of carbamazepine and its derivatives, oxcarbazepine, BIA 2–093, and BIA 2–024. Neurochem. Res. 27, 121–130.
Ana, R., Mendes, M., Sousa, J., Pais, A., Falcão, A., Fortuna, A., Vitorino, C., 2019. Rethinking carbamazepine oral delivery using polymer-lipid hybrid nanoparticles. Int. J. Pharm. 554, 352–365.
Anton, N., Benoit, J.-P., Saulnier, P., 2008. Design and production of nanoparticles formulated from nano-emulsion templates- A review. J. Control. Release 128, 185–199.
Barakat, N.S., Omar, S.A., Ahmed, A.A., 2006. Carbamazepine uptake into rat brain following intra-olfactory transport. J. Pharm. Pharmacol. 58, 63–72.
Baratchi, S., Kanwar, R.K., Khoshmanesh, K., Vasu, P., Ashok, C., Hittu, M., Parratt, A., Krishnakumar, S., Sun, X., Sahoo, S.K., Kanwar, J.R., 2009. Promises of nanotechnology for drug delivery to brain in neurodegenerative diseases. Curr. Nanosci. 5, 15–25.
Blasi, P., Giovagnoli, S., Schoubben, A., Ricci, M., Rossi, C., 2007. Solid lipid nanoparticles for targeted brain drug delivery. Adv. Drug Deliv. Rev. 59, 454–477.
Bourin, M., 2015. Animal models for screening anxiolytic-like drugs: a perspective. Dialogues Clin. Neurosci. 17, 295–303.
Bourin, M., Hascoët, M., 2003. The mouse light/dark box test. Eur. J. Pharmacol. 463, 55–65.
Chen, C., Tan, R., Qu, W., Wu, Z., Wang, Y., Urade, Y., Huang, Z., 2011. Magnolol, a major bioactive constituent of the bark of Magnolia officinalis, exerts antiepileptic effects via the GABA/benzodiazepine receptor complex in mice. Br. J. Pharmacol. 164, 1534–1546.
Chen, W., Gu, B., Wang, H., Pan, J., Lu, W., Hou, H., 2008. Development and evaluation of novel itraconazole-loaded intravenous nanoparticles. Int. J. Pharm. 362, 133–140.
Din, F.U., Aman, W., Ullah, I., Qureshi, O.S., Mustapha, O., Shafique, S., Zeb, A., 2017. Effective use of nanocarriers as drug delivery systems for the treatment of selected tumors. Int. J. Nanomedicine 12, 7291–7309.
Din, F.U., Zeb, A., Shah, K.U., Ziaur, R., 2019. Development, in-vitro and in-vivo evaluation of ezetimibe-loaded solid lipid nanoparticles and their comparison with marketed product. J. Drug Deliv. Sci. Technol. 51, 583–590.
Elmowafy, M., Shalaby, K., Badran, M.M., Ali, H.M., Abdel-Bakky, M.S., Ibrahim, H.M., 2018. Multifunctional carbamazepine loaded nanostructured lipid carrier (NLC) formulation. Int. J. Pharm. 550, 359–371.
Estella-Hermoso de Mendoza, A., Campanero, M.A., Mollinedo, F., Blanco-Prieto, M.J., 2009. Lipid nanomedicines for anticancer drug therapy. J. Biomed. Nanotechnol. 5, 323–343.
Etame, A.B., Smith, C.A., Chan, W.C.W., Rutka, J.T., 2011. Design and potential application of PEGylated gold nanoparticles with size-dependent permeation through brain microvasculature. Nanomedicine 7, 992–1000.
Gabathuler, R., 2010. Approaches to transport therapeutic drugs across the blood–brain barrier to treat brain diseases. Neurobiol. Dis. 37, 48–57.
Goldsmith, M., Abramovitz, L., Peer, D., 2014. Precision nanomedicine in neurodegenerative diseases. ACS Nano 8, 1958–1965.
He, X., Zhu, Y., Wang, M., Jing, G., Zhu, R., Wang, S., 2016. Antidepressant effects of curcumin and HU-211 coencapsulated solid lipid nanoparticles against corticosterone-induced cellular and animal models of major depression. Int. J. Nanomed. 11, 4975–4990.
Hu, F.-Q., Jiang, S.-P., Du, Y.-Z., Yuan, H., Ye, Y.-Q., Zeng, S., 2005. Preparation and characterization of stearic acid nanostructured lipid carriers by solvent diffusion method in an aqueous system. Colloids Surf. B: Biointerfaces 45, 167–173.
Islan, G.A., Tornello, P.C., Abraham, G.A., Duran, N., Castro, G.R., 2016. Smart lipid nanoparticles containing levofloxacin and DNase for lung delivery. Design and characterization. Colloids Surf. B: Biointerfaces 143, 168–176.
Karim, N., Curmi, J., Gavande, N., Johnston, G.A., Hanrahan, J.R., Tierney, M.L., Chebib, M., 2012. 2′-Methoxy-6-methylflavone: a novel anxiolytic and sedative with subtype selective activating and modulating actions at GABAA receptors. Br. J. Pharmacol. 165, 880–896.
Kaur, I.P., Bhandari, R., Bhandari, S., Kakkar, V., 2008. Potential of solid lipid nanoparticles in brain targeting. J. Control. Release 127, 97–109.
Khan, A.W., Khan, A.U., Ahmed, T., 2016. Anticonvulsant, anxiolytic, and sedative activities of Verbena officinalis. Front. Pharmacol. 7, 499.
Kumar, R., Siril, P.F., 2014. Ultrafine carbamazepine nanoparticles with enhanced water solubility and rate of dissolution. RSC Adv. 4, 48101–48108.
Kwan, P., Brodie, M.J., 2005. Potential role of drug transporters in the pathogenesis of medically intractable epilepsy. Epilepsia 46, 224–235.
Landmark, C.J., Johannessen, S.I., Tomson, T., 2012. Host factors affecting antiepileptic drug delivery—Pharmacokinetic variability. Adv. Drug Deliv. Rev. 64, 896–910.
Li, B., Wang, L., Sun, Z., Zhou, Y., Shao, D., Zhao, J., Song, Y., Lv, J., Dong, X., Liu, C., Wang, P., Zhang, X., Cui, R., 2014. The anticonvulsant effects of SR 57227 on pentylenetetrazole-induced seizure in mice. PLoS One 9, e93158.
Lim, W.M., Rajinikanth, P.S., Mallikarjun, C., Kang, Y.B., 2014. Formulation and delivery of itraconazole to the brain using a nanolipid carrier system. Int. J. Nanomed. 9, 2117–2126.
Liu, S., Yang, S., Ho, P.C., 2018. Intranasal administration of carbamazepine-loaded carboxymethyl chitosan nanoparticles for drug delivery to the brain. Asian J. Pharm. Sci. 13, 72–81.
Lockman, P.R., Koziara, J.M., Mumper, R.J., Allen, D.D., 2004. Nanoparticle surface charges alter blood-brain barrier integrity and permeability. J. Drug Target. 12, 635–641.
Lv, Q., Yu, A., Xi, Y., Li, H., Song, Z., Cui, J., Cao, F., Zhai, G., 2009. Development and evaluation of penciclovir-loaded solid lipid nanoparticles for topical delivery. Int. J. Pharm. 372, 191–198.
Mesdaghinia, A., Alinejad, M., Abed, A., Heydari, A., Banafshe, H.R., 2019. Anticonvulsant effects of thiamine on pentylenetetrazole-induced seizure in mice. Nutr. Neurosci. 22, 165–173.
Müller, R.H., Radtke, M., Wissing, S.A., 2002. Nanostructured lipid matrices for improved microencapsulation of drugs. Int. J. Pharm. 242, 121–128.
Qureshi, O.S., Kim, H.-S., Zeb, A., Choi, J.-S., Kim, H.-S., Kwon, J.-E., Kim, M.-S., Kang, J.-H., Ryou, C., Park, J.-S., Kim, J.-K., 2017. Sustained release docetaxel-incorporated lipid nanoparticles with improved pharmacokinetics for oral and parenteral administration. J. Microencapsul. 34, 250–261.
Qureshi, O.S., Zeb, A., Akram, M., Kim, M.-S., Kang, J.-H., Kim, H.-S., Majid, A., Han, I., Chang, S.-Y., Bae, O.-N., Kim, J.-K., 2016. Enhanced acute anti-inflammatory effects of CORM-2-loaded nanoparticles via sustained carbon monoxide delivery. Eur. J. Pharm. Biopharm. 108, 187–195.
Rizvi, S.Z.H., Shah, F.A., Khan, N., Muhammad, I., Ali, K.H., Ansari, M.M., Din, F.U., Qureshi, O.S., Kim, K.W., Choe, Y.H., Kim, J.K., Zeb, A., 2019. Simvastatin-loaded solid lipid nanoparticles for enhanced anti-hyperlipidemic activity in hyperlipidemia animal model. Int. J. Pharm. 560, 136–143.
Saraiva, C., Praca, C., Ferreira, R., Santos, T., Ferreira, L., Bernardino, L., 2016. Nanoparticle-mediated brain drug delivery: Overcoming blood-brain barrier to treat neurodegenerative diseases. J. Control. Release 235, 34–47.
Scioli Montoto, S., Sbaraglini, M.L., Talevi, A., Couyoupetrou, M., Di Ianni, M., Pesce,

G.O., Alvarez, V.A., Bruno-Blanch, L.E., Castro, G.R., Ruiz, M.E., Islan, G.A., 2018. Carbamazepine-loaded solid lipid nanoparticles and nanostructured lipid carriers: Physicochemical characterization and in vitro/in vivo evaluation. Colloids Surf. B: Biointerfaces 167, 73–81.
Sethia, S., Squillante, E., 2002. Physicochemical characterization of solid dispersions of carbamazepine formulated by supercritical carbon dioxide and conventional solvent evaporation method. J. Pharm. Sci. 91, 1948–1957.
Sim, T., Lim, C., Hoang, N.H., Joo, H., Lee, J.W., Kim, D.-W., Lee, E.S., Youn, Y.S., Kim, J.O., Oh, K.T., 2016. Nanomedicines for oral administration based on diverse nano-platform. J. Pharm. Investig. 46, 351–362.
Sperling, M.R., 2004. The consequences of uncontrolled epilepsy. CNS Spectr. 9, 98–101 106–109.
Tapeinos, C., Battaglini, M., Ciofani, G., 2017. Advances in the design of solid lipid nanoparticles and nanostructured lipid carriers for targeting brain diseases. J. Control. Release 264, 306–332.
Üner, M., Yener, G., 2007. Importance of solid lipid nanoparticles (SLN) in various administration routes and future perspectives. Int. J. Nanomedicine 2, 289–300.
Van Calker, D., Steber, R., Klotz, K.N., Greil, W., 1991. Carbamazepine distinguishes between adenosine receptors that mediate different second messenger responses. Eur. J. Pharmacol. 206, 285–290.
Walf, A.A., Frye, C.A., 2007. The use of the elevated plus maze as an assay of anxiety-related behavior in rodents. Nat. Protoc. 2, 322–328.
Wen, Z., Yan, Z., He, R., Pang, Z., Guo, L., Qian, Y., Jiang, X., Fang, L., 2011. Brain targeting and toxicity study of odorranalectin-conjugated nanoparticles following intranasal administration. Drug Deliv. 18, 555–561.
WHO, 2019. Epilepsy fact sheet. Available from: https://www.who.int/en/news-room/fact-sheets/detail/epilepsy. [Accessed 28-06-2019].
Wiebe, S., Jette, N., 2012. Pharmacoresistance and the role of surgery in difficult to treat epilepsy. Nature Rev. Neurol. 8, 669–677.
Wong, H.L., Chattopadhyay, N., Wu, X.Y., Bendayan, R., 2010. Nanotechnology applications for improved delivery of antiretroviral drugs to the brain. Adv. Drug Deliv. Rev. 62, 503–517.
Zeb, A., Arif, S.T., Malik, M., Shah, F.A., Din, F.U., Qureshi, O.S., Lee, E.-S., Lee, G.-Y., Kim, J.-K., 2019a. Potential of nanoparticulate carriers for improved drug delivery via skin. J. Pharm. Investig. 49, 485–517.
Zeb, A., Cha, J.-H., Noh, A.R., Qureshi, O.S., Kim, K.-W., Choe, Y.-H., Shin, D., Shah, F.A., Majid, A., Bae, O.-N., Kim, J.-K., 2019b. Neuroprotective effects of carnosine-loaded elastic liposomes in cerebral ischemia rat model. J. Pharm. Investig.
Zeb, A., Qureshi, O.S., Kim, H.S., Cha, J.H., Kim, H.S., Kim, J.K., 2016. Improved skin permeation of methotrexate via nanosized ultradeformable liposomes. Int. J. Nanomed. 11, 3813–3824.
Zeb, A., Qureshi, O.S., Kim, H.S., Kim, M.S., Kang, J.H., Park, J.S., Kim, J.K., 2017. High payload itraconazole-incorporated lipid nanoparticles with modulated release property for oral and parenteral administration. J. Pharm. Pharmacol. 69, 955–966.
Zhang, J., Fan, Y., Smith, E., 2009. Experimental design for the optimization of lipid nanoparticles. J. Pharm. Sci. 98, 1813–1819.
Zheng, Y., Zheng, M., Ma, Z., Xin, B., Guo, R., Xu, X., 2015. 8 - Sugar fatty acid esters. In: Ahmad, M.U., Xu, X. (Eds.), Polar Lipids. Elsevier, pp. 215–243.
Zybina, A., Anshakova, A., Malinovskaya, J., Melnikov, P., Baklaushev, V., Chekhonin, V., Maksimenko, O., Titov, S., Balabanyan, V., Kreuter, J., Gelperina, S., Abbasova, K., 2018. Nanoparticle-based delivery of carbamazepine: A promising approach for the treatment of refractory epilepsy. Int. J. Pharm. 547, 10–23.